Original Article

MOLECULAR METABOLISM

Genetically-encoded sensors to detect fatty acid production and trafficking

Emilio P. Mottillo [1,*,2], Huamei Zhang [1], Alexander Yang [1], Li Zhou [1], James G. Granneman [1]

ABSTRACT

Objective: Fatty acids are important for biological function; however, in excess, they can cause metabolic dysregulation. Methods to image and detect fatty acids in real time are lacking. Therefore, the current study examined the dynamics of fatty acid trafficking and signaling utilizing novel fluorescent and luminescent approaches.

Methods: We generated fluorescent and luminescent-based genetically-encoded sensors based upon the ligand-dependent interaction between PPARα and SRC-1 to image and detect cellular dynamics of fatty acid trafficking.

Results: The use of a fluorescent sensor demonstrates that fatty acids traffic rapidly from lipid droplets to the nucleus. Both major lipases ATGL and HSL contribute to fatty acid signaling from lipid droplet to nucleus, however, their dynamics differ. Furthermore, direct activation of lipolysis, independent of receptor-mediated signaling is sufficient to promote lipid droplet to nuclear trafficking of fatty acids. A luminescent-based sensor that reports intracellular fatty acid levels is amenable to high-throughput analysis.

Conclusions: Fatty acids traffic from lipid droplets to the nucleus within minutes of stimulated lipolysis. Genetically-encoded fluorescent and luminescent based sensors can be used to probe the dynamics of fatty acid trafficking and signaling.

© 2019 The Authors. Published by Elsevier GmbH. This is an open access article under the CC BY-NC-ND license (http://creativecommons.org/licenses/by-nc-nd/4.0/).

Keywords Lipolysis; Brown adipocyte; Lipid droplet; Luminescent sensor; Fluorescent sensor; Fatty acid

1. INTRODUCTION

Fatty acids (FAs) are a significant energy source and substrates for membrane synthesis that are required for cellular growth and division. Importantly, recent work has identified a role for FAs as signaling molecules in regulating lipid homeostasis [1]. On the other hand, excessive levels of FAs can lead to a build up of toxic lipid metabolic intermediates in a process termed lipotoxicity [2]. This buildup of lipids can have negative effects that are causative in various metabolic disorders, such as diabetes [3] and cardiovascular disease [4]. However, our understanding of FA metabolism has been hampered by the lack of methods to detect their production in a temporal and spatial manner in live cells.

FAs are stored safely in the form of triacylglycerol (TAG) within lipid droplet (LD) organelles [5]. During times of energy demand these stores are mobilized by lipases on the surface of LDs. In adipocytes, this process is mediated by the major lipases adipose triglyceride lipase (ATGL; also known as Patatin Like Phospholipase Domain Containing 2, PNPLA2), the rate limiting enzyme for TAG hydrolysis and hormone sensitive lipase (HSL), a major diacylglycerol (DAG) lipase [6]. In brown adipocytes (BAs), FAs are essential regulators of thermogenesis [7,8] by supplying energy for mitochondrial electron transport and functioning as allosteric activators of uncoupling protein 1 (UCP1) [9], the molecular mechanisms for brown adipose tissue non-shivering thermogenesis.

Recent work has demonstrated that ATGL and HSL can regulate the transcription of various genes involved in FA metabolism and uncoupling such as peroxisome proliferator-activated receptor gamma coactivator 1-alpha (PGC1α), pyruvate dehydrogenase kinase 4 (PDK4), and UCP1, likely by providing ligands for nuclear transcription factors peroxisome proliferator-activated receptors (PPARs) [10–13]. However, the temporal and spatial regulation of how FAs might traffic to promote gene expression is not known. In addition, methods to detect real time mobilization of intracellular FAs are lacking. Here we describe the development of genetically-encoded sensors based upon the ligand-dependent interaction between PPARα and steroid receptor coactivator-1 (SRC-1) to image the production and trafficking of FAs by fluorescent and luminescent means.

2. METHODS AND EXPERIMENTAL PROCEDURES

2.1. cDNA cloning and generation of cell lines

Cloning for the PPARα ligand binding domain (LBD) and the SRC-1 fragment were previously described [10]. Briefly, the bipartite FA sensor was generated by first cloning the LXXLL domain of SRC-1 (amino acids, aa; 620–770) on the C-terminus of EYFP (Clontech). The LBD of human PPARα (aa 191–467) was cloned on the C-

[1]Center for Molecular Medicine and Genetics, Wayne State University School of Medicine, Detroit, MI, 48201, USA

[2] Current Address: Henry Ford Hospital, Department of Internal Medicine, Hypertension and Vascular Research Division, Detroit, MI, 48202, USA.

*Corresponding author. Henry Ford Hospital, Hypertension and Vascular Research Division, Education and Research Building, 7089, 2799 W. Grand Blvd., Detroit, MI, 48202, USA. E-mail: emottil1@hfhs.org (E.P. Mottillo).

Received July 5, 2019 • Revision received August 9, 2019 • Accepted August 14, 2019 • Available online 20 August 2019

https://doi.org/10.1016/j.molmet.2019.08.012

 © 2019 The Authors. Published by Elsevier GmbH. This is an open access article under the CC BY-NC-ND license (http://creativecommons.org/licenses/by-nc-nd/4.0/).

Abbreviations

ABHD5	Alpha-beta hydrolase domain-containing 5
Ai	Atglistatin
ATGL	Adipose triglyceride lipase
BA	Brown adipocyte
BAY	BAY 59-9435
BSA	Bovine serum albumin
DAG	Diacylglycerol
Dox	Doxycycline
FA	Fatty acid
Gluc	*Gaussia* luciferase
HSL	hormone sensitive lipase
HTS	High-throughput screening
LBD	ligand binding domain
LD	lipid droplet
PDK4	Pyruvate dehydrogenase kinase 4
PKA	Protein kinase A
PGC1α	peroxisome proliferator-activated receptor gamma coactivator 1-alpha
PLIN1	Perilipin-1
PNPLA2	Patatin Like Phospholipase Domain Containing 2
PPARs	Peroxisome proliferator-activated receptors
RLUs	Relative Luminescence Units
ROI	Region of interest
SRC-1	Steroid receptor coactivator-1
TAG	Triacylglycerol
UCP1	Uncoupling protein 1

terminus of full-length Perilipin-1 (PLIN1). The PLIN1- PPARα LBD fusion was then sub-cloned on the C-terminus of EYFP-SRC1 separated by a P2A sequence.

The cDNA for a monomeric luciferase FA sensor was commercially synthesized (Genewiz Inc.). Briefly, *Gaussia* luciferase (Gluc) was split into optimized N-terminal (aa 18—105; GlucN) and C-terminal fragments (aa 106—185; GlucC) as previous described [14]. The GlucN fragment was followed by the LBD of PPARα, the LXXLL motif of SRC-1 and finally the GlucC fragment. Each fragment was separated by flexible linkers 2X(Gly-Gly-Gly-Gly-Ser). The synthesized DNA fragment containing AgeI and XbaI sites was cloned into the same sites of ECFP-C1.

The indicated constructs were cloned into the lentivirus vector (pINDUCER20) as previously described [15,16]. For lentiviral packaging, pINDUCER20 target plasmid was co-transfected with pMD2.G and psPAX2 packaging vectors into HEK293T cells using lipofectamine LTX and plus reagent (Invitrogen). 48 h and 72 h post transfection, virus-containing culture media was harvested and passed through 0.45 μM filters to remove debris. To collect the virus, the media was centrifuged at 48,000× *g* for 2 h 4 °C in a Beckman 25.50 fixed angle rotor, and the virus pellet was resuspended in OPTIMEM. Stable brown adipocyte (BA) cells line expressing sensors were generated by infecting with virus for 24 h followed by G418 selection (800 μg/ml) for one week.

2.2. Cell culture

HEK293T and COS-7 cells were purchased from ATCC. Mouse brown preadipocyte cells lines were generated in the labs of Dr. Bruce Spiegelman (Harvard University) or Dr. Gregory Steinberg (McMaster University) and were provided as gifts. All cells were maintained in DMEM High Glucose (Hyclone GE Lifesciences) with 10% FCS (Atlanta Biologicals) and Penicillin/Streptomycin (Hyclone, GE Lifesciences). Brown preadipocytes were differentiated by treating cells with induction medium (20 nM insulin, 1 nM T3, 0.5 mM isobutylmethylxanthine, 0.5 μM dexamethasone, and 0.125 mM indomethacin) for 48 h, followed by maintenance in differentiation media (20 nM insulin, 1 nM T3) until complete differentiation at 7 days. The expression of stably integrated sensors was induced by treating cells with 1 μg/ml doxycycline for 24—48 h.

2.3. Microscopy

Images were acquired using an Olympus IX-81 microscope equipped with a spinning-disc confocal unit. Microscope control and data acquisition were performed using CellSens Dimensions (Olympus) software. BAs grown and differentiated on 35 mm glass coverslips were imaged in HEPES-Krebs-Ringer buffer (Sigma) supplemented with 1% BSA (Alkali Scientific). EYFP fluorescent images were acquired using a 40 × (0.9 NA) or 60 × (1.2 NA) water immersion lens. EYFP reporter images were acquired every minute, with basal fluorescence recorded for the first 3—5 min, followed by stimulation of lipolysis (forskolin/IBMX, 2 μM and 200 μM; ABHD5 ligand; isoproterenol). The region of interest (ROI; lipid droplets, nucleus or cytoplasm) for each frame was quantified using ImageJ software (NIH) and the LD or nucleus ROI was normalized to cytoplasm to correct for any nonspecific changes in fluorescent intensity due to minor changes in excitation or focal plane. Data were then expressed as a fold of basal fluorescence.

2.4. Immunofluorescence

BAs grown on 35 mm glass coverslips were induced to express the fluorescent FA sensor for 48 h. Cells were treated with vehicle or Isoproterenol for 20 min as above for microscopy experiments. Fixed cells were permeabilized with phosphate-buffered saline containing 5% normal donkey serum and 0.01% saponin (Permeabilization buffer) for 15 min, then incubated for 50 min in Permeabilization buffer with primary antibody against PLIN1 (goat, 1:200, Everest Biotech, Cat# EB07728). The slides were washed four times, 5 min each, with phosphate-buffered saline, then incubated for 1 h with Alexa Fluor 555 conjugated donkey anti-goat (1:1000; Invitrogen) in Permeabilization buffer. The slides were washed again, then counterstained for nuclei (4′,6-diamidino-2-phenylindole; 1:5000) in phosphate-buffered saline. Slides were finally washed with phosphate-buffered saline and imaged as above on an Olympus IX-81.

2.5. Gene expression analysis

RNA was isolated from BAs using a Nucleospin RNA II kit (Machery-Nagel) as indicated by the manufacturer. Total RNA was reverse transcribed using Superscript III (Invitrogen) with oligo(dT) primers (ThermoFisher). Fifty nanograms of cDNA was analyzed in a 20-μl quantitative PCR reaction (ABsolute Blue QPCR SYBR; ThermoScientific) with 80 nM of primers. Expression data were normalized to the housekeeping gene peptidylprolyl *cis—trans* isomerase A (PPIA) using the $\Delta\Delta C_T$ method ($2^{-\Delta\Delta CT}$) [17]. cDNAs were amplified using primers as previously described [10].

2.6. Luciferase assays

Immediately following treatments, cells were washed once with PBS and luciferase assays were performed by lysing cells in Gluc assay

 © 2019 The Authors. Published by Elsevier GmbH. This is an open access article under the CC BY-NC-ND license (http://creativecommons.org/licenses/by-nc-nd/4.0/).

buffer (30 mM Tris pH 8.0, 300 mM NaCl, 0.1% Tween 20) [18] for 20 min at room temperature with gentle rotation. Luciferase activity was measured by injecting coelenterazine (20 μM) in PBS and measuring luminescence over a 2 s integration.

2.7. Biochemical measurements

Fatty acids released in the media were determined using a WAKO NEFA HR kit (Wako Pure Chemicals Industries) adapted to fluorescence detection with Amplex Red (Cayman Chemical). Glycerol was quantified using the Free Glycerol (Sigma) reagent with colorimetric determination.

3. RESULTS

3.1. Fluorescent imaging reveals dynamic trafficking of fatty acids from lipid droplets to nucleus

We previously described a fluorescent method to monitor the production of PPARα and PPARδ ligands on LDs [10]. This assay involves targeting the ligand binding domain (LBD) of PPARα to the LD surface by fusing it to Perilipin 1 (PLIN1) and tagging the LxxLL motif of SRC-1 with EYFP. The presence of a FA (*i.e.*, PPAR ligand) promotes the ligand dependent interaction between PPARα and SRC-1, which can be monitored by the accumulation of fluorescence at the LD surface. In addition to monitoring ligand production to genetically-targeted PPARα LBD, translocation of tagged SRC1 to endogenous nuclear receptors could provide a means of monitoring FA-induced transactivation in real time. To improve on the original design [10], we incorporated the targeted LBD and fluorescent co-activator reporter into a single transcript using the P2A peptide to control relative expression levels. Furthermore, we put the construct under the control of a doxycycline inducible promoter (Figure 1A) and created a stable BA cell line that allowed controlled expression to detect the ligand dependent interaction (Figure 1B). In BA cells treated with doxycycline, EYFP-SRC-1 fluorescence was localized throughout the cytosol with some nuclear localization. Upon activation of protein kinase A (PKA) with forskolin/IBMX to stimulate lipolysis, fluorescent EYFP-SRC1 rapidly translocated to the LD surface (arrowheads; Figure 1C,D, Supplementary Movie 1), indicating that PPARα ligands (i.e. fatty acids) are immediately produced from LDs upon stimulation of lipolysis. Quantification of regions of interest (ROI) demonstrated a robust increase in EYFP fluorescence on the LD that occurred within 1–3 min of stimulating lipolysis. This early burst in the accumulation of EYFP was followed by a steady continuous accumulation in signal (Figure 1E). Somewhat unexpectedly, we also observed accumulation of EYFP-SRC1 within the nucleus (black arrows). The accumulation of EYFP-SRC1 in the nucleus steadily increased over 15 min and lacked the rapid phase observed at the LD

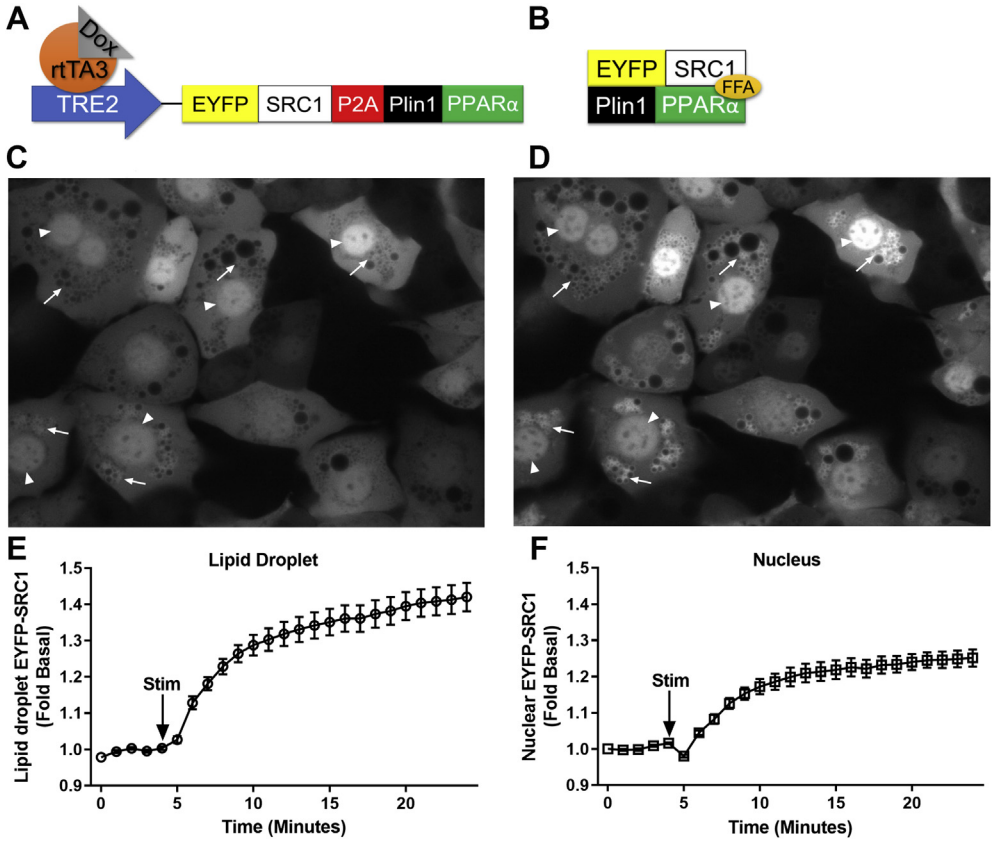

Figure 1: Design of a fluorescent sensor to detect fatty acid trafficking on lipid droplets and in the nucleus. (**A**) Schematic for the design of a doxycycline (Dox) inducible bipartite fluorescent sensor to detect fatty acids. The co-activation domain of SRC1 is tagged to EYFP (EYFP-SRC1), separated by a P2A self-cleaving site with PLIN1-PPARα fusion, which targets the ligand binding domain of PPARα to lipid droplets. Dox binds reverse tetracycline-controlled transactivator (rtTA3), which promotes binding to the TRE2 promoter to induce expression of the fatty acid sensor. (**B**) In the presence of ligand (fatty acid; FFA), EYFP-SRC1 binds to PLIN1-PPARα on the surface of LDs. EYFP-SRC1 can also translocate to endogenous nuclear receptors that are sensitive to fatty acids. Stable expression of the fluorescent fatty acid reporter in brown adipocytes under basal conditions (**C**) and protein kinase A (PKA) stimulation (Stim; forskolin/IBMX) for 20 min (**D**). Arrows note accumulation of EYFP-SRC1 on lipid droplets while arrowheads note accumulation within the nucleus following stimulation. Quantification of the region of interest on lipid droplet (**E**) and nucleus (**F**) normalized to the cytosol signal and expressed as fold of basal.

 © 2019 The Authors. Published by Elsevier GmbH. This is an open access article under the CC BY-NC-ND license (http://creativecommons.org/licenses/by-nc-nd/4.0/).

surface (Figure 1F). We confirmed using immunofluorescence that the PLIN1-PPARα fusion remains on LD during stimulation (Supplementary Figure 1). Thus, the translocation of EYFP-SRC1 to the nucleus most likely represents the FA-dependent interaction of EYFP-SRC1 with endogenous nuclear receptors (Supplementary Figure 1). These data demonstrate the rapid mobilization of FAs on LDs and their detection in the nucleus.

Supplementary video related to this article can be found at https://doi.org/10.1016/j.molmet.2019.08.012

ATGL and HSL are the major adipocyte lipases which differ in their targeted substrates and mode of activation [6,19]. In the basal state ATGL has weak TAG lipase activity; however, PKA activation phosphorylates PLIN1 to release the co-activator alpha-beta hydrolase domain-containing 5 (ABHD5, also known as CGI-58) [20], which then activates ATGL [19]. In contrast, HSL is directly phosphorylated by PKA, which targets the lipase to LD surfaces and increases its activity [21,22]. Both ATGL and HSL contribute to adipocyte lipolysis, acting as selective TAG and DAG lipases, respectively, yet how these lipases contribute the temporal and spatial mobilization of FAs has not been investigated. As shown in Figure 2A, activation of β-adrenergic receptors with isoproterenol (Iso) triggered a burst of EYFP-SRC1 fluorescence on LD surfaces within 2 min of activation, followed by a steady increase over the next 15 min. Pharmacological inhibition of HSL with BAY 59−9435 (BAY) [23] eliminated the rapid rise in fluorescence associated with LDs, but left largely intact the slower rise observed in control cells. Conversely, the rapid phase of FA mobilization was intact in the presence of ATGL inhibition with Atglistatin (Ai) [24], yet enduring mobilization of FAs was largely eliminated in the absence of ATGL activity (Figure 2A). These observations indicate that HSL can mediate a very rapid mobilization of FAs, and that ATGL is critical for sustained mobilization. Furthermore, results indicate that both lipases function in concert to achieve a full lipolytic response, consistent with experiments that monitor extracellular accumulation of FAs (Supplementary Figure 2).

Fluorescent-tagged SRC-1 accumulation in the nucleus showed somewhat different kinetics, with no detectible burst and a slow accumulation that was similarly sensitive to inhibition of ATGL or HSL (Figure 2B). Consistent with the notion that ATGL and HSL are the

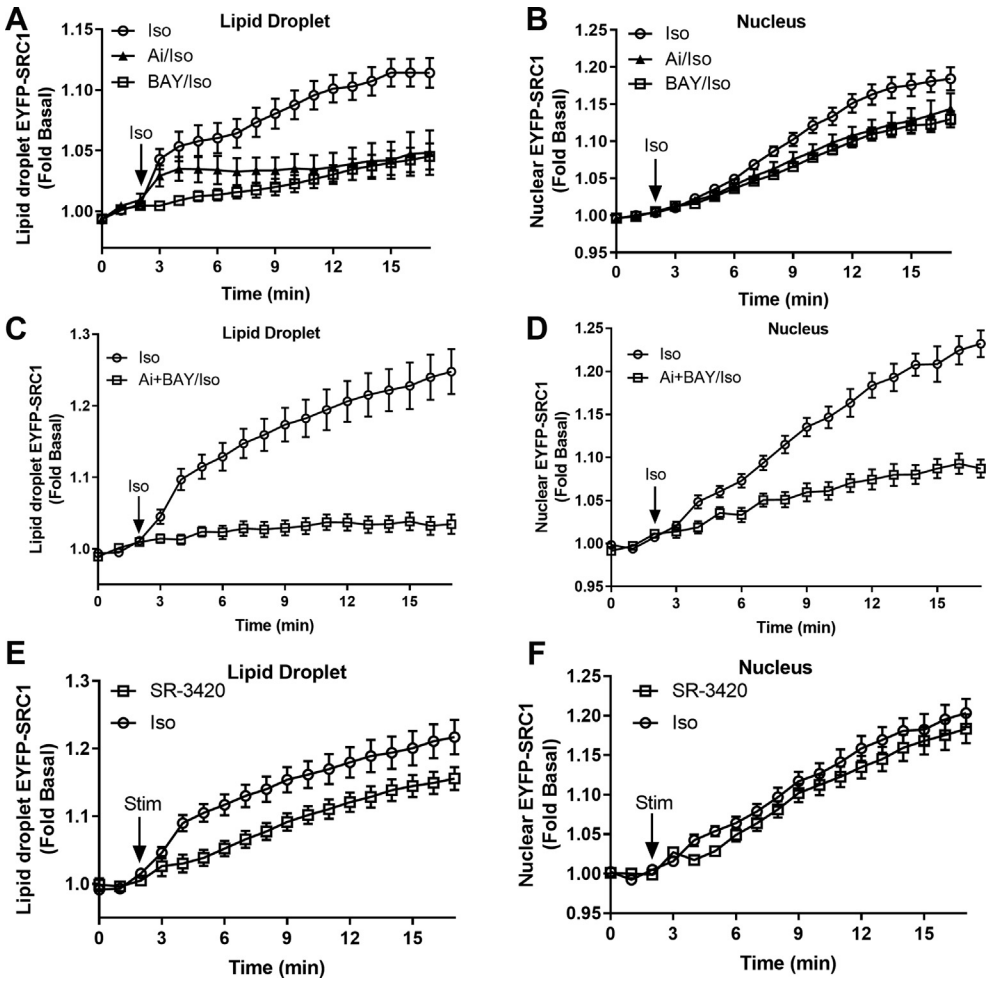

Figure 2: Role of ATGL, HSL and ABHD5 in fatty acid trafficking from lipid droplets and in the nucleus. Individual contribution of ATGL and HSL to fatty acid signaling on lipid droplets (**A**) and in the nucleus (**B**). Combined contribution of both ATGL and HSL to fatty acid signaling on lipid droplets (**C**) and in the nucleus (**D**). Cell were pretreated with DMSO (in the case for Iso alone) or in the presence of ATGL inhibitor (Ai, 10 μM), HSL inhibitor (BAY, 5 μM), or both inhibitors for 20 min, then imaged basally for three minutes, followed by stimulation with isoproterenol (Iso, 1 μM) for 15 min. Role of direct ABHD5 activation on fatty acid signaling on lipid droplets (**E**) and in the nucleus (**F**). Brown adipocytes were imaged basally for 3 min followed by stimulation with Isoproterenol (Iso, 1 μM) or ABHD5 activation (SR-3420, 20 μM) for 15 min. The region of interest on lipid droplet, nucleus was quantified and normalized to the cytosol signal and expressed as fold of basal.

 © 2019 The Authors. Published by Elsevier GmbH. This is an open access article under the CC BY-NC-ND license (http://creativecommons.org/licenses/by-nc-nd/4.0/).

major adipocyte lipases, dual inhibition of ATGL and HSL completely blocked the accumulation of EYFP-SRC1 (Figure 2C) on LDs and reduced accumulation in the nucleus by greater than 80% (Figure 2D). These data demonstrate that FAs can traffic from the LD to the nucleus through the function of ATGL and HSL and that these enzymes differ in their kinetics of FA mobilization on LDs.

The results with lipase inhibition indicate that PKA-induced HSL activation mediates rapid FA mobilization, whereas the sustained phase of LD-mediated FA signaling requires ATGL that might be independent of transmembrane signaling. To address the role of PKA activation in the temporal control of lipolysis, we compared receptor mediated-activation by Iso with that induced by ABHD5 ligands, which activate ATGL-dependent lipolysis directly [15,25]. These ligands stimulate lipolysis by binding ABHD5, reducing its affinity for PLIN1, thereby stimulating ATGL-dependent lipolysis independently of PKA. As expected, Iso promoted the increase in EYFP-SRC1 with two distinct phases, while direct activation of ABHD5 with SR-3420 promoted the steady accumulation of EYFP-SRC1 on the LD surface that lacked the initial burst observed with receptor activation (Figure 2E). Interestingly, the profile of EYFP-SRC1 accumulation on LDs triggered by SR-3420 mimicked that of receptor mediated lipolysis when it was driven exclusively by ATGL (Figure 2A, BAY/Iso). The accumulation of EYFP-SRC1 within the nucleus was similar whether lipolysis was induced via activation of β-adrenergic receptors with isoproterenol or triggered by activation of ABHD5 with SR-3420 (Figure 2F). Overall, these results demonstrate that direct activation of lipolysis is sufficient to promote FA trafficking from LDs to the nucleus.

The accumulation of EYFP-SRC1 within the nucleus suggested that FAs might traffic to the nucleus to modulate gene transcription via endogenous nuclear receptors. Because the fragment of SRC-1 used as a reporter lacks the activation domain, we reasoned that binding of this reporter to endogenous transcription factors might function as a dominant-negative to suppress the transcription of genes responsive to FA production. As shown in Figure 3A, Iso increased the expression of known PPAR target genes that are involved in fatty acid oxidation (PGC1α, PPARα, PDK4) and UCP1. Furthermore, doxycycline-induced expression of EYFP-SRC1 (+Dox) lowered the expression of these genes but not expression of NOR-1 [10], a direct PKA target gene. (Figure 3A). Importantly, the expression of the SRC-1 fragment did not affect the release of FAs (Supplementary Figure 3). Overall, these results indicate a LD to nucleus pathway that communicates the metabolic status of the cell to rapidly regulate the expression of genes involved in fatty acid oxidation and uncoupling.

3.2. A high throughput luciferase-based sensor to detect intracellular fatty acids

The fluorescent reporter provides local information on FA signaling. We next sought to determine whether the sensor system described could be adapted for high-throughput screening (HTS). To do so, we engineered luciferase complementation based on optimized fragments for a split *Gaussia* luciferase (Gluc) [26] into a single genetically-encoded reporter (Figure 4A). In HEK 293T cells transiently transfected with the luciferase sensor, the addition of PPAR ligands resulted in an increase in luciferase signal in response to PPARα ligands Wy14-643 (Wy) and GW7647, but not PPARγ ligand rosiglitazone (Figure 4B). A dose response for Wy resulted in a calculated EC_{50} of 0.54 μM, similar to the reported EC_{50} values for this ligand (Figure 4C) [27,28]. Overall, these results demonstrate that the luminescent based sensor is selectively responsive to PPARα ligands.

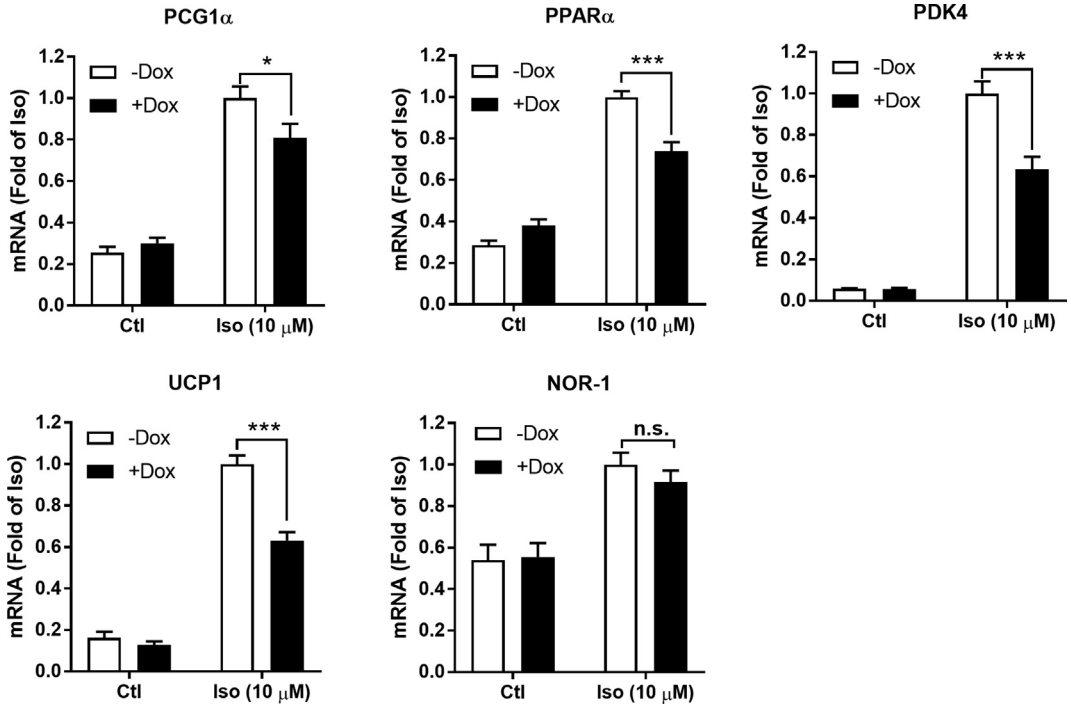

Figure 3: The dominant-negative fragment of SRC-1 suppresses the induction of known PPAR target genes. Brown adipocyte cells stably expressing the SRC-1 fragment in a doxycycline-inducible manner were treated with (+Dox) or without (-Dox) doxycycline (1 μg/ml) for 48 h, followed by vehicle (Ctl) or Isoproterenol (Iso, 10 μM) for four hours. The RNA was extracted, and the expression of the indicated genes was measured. *$p < 0.05$ and ***$p < 0.001$ indicate a significant effect of doxycycline-induced expression of EYFP-SRC-1 on the expression of genes induced by isoproterenol treatment (Iso) as determine by two-way ANOVA with Bonferroni post t-test. n.s. indicates a non-significant effect.

 © 2019 The Authors. Published by Elsevier GmbH. This is an open access article under the CC BY-NC-ND license (http://creativecommons.org/licenses/by-nc-nd/4.0/).

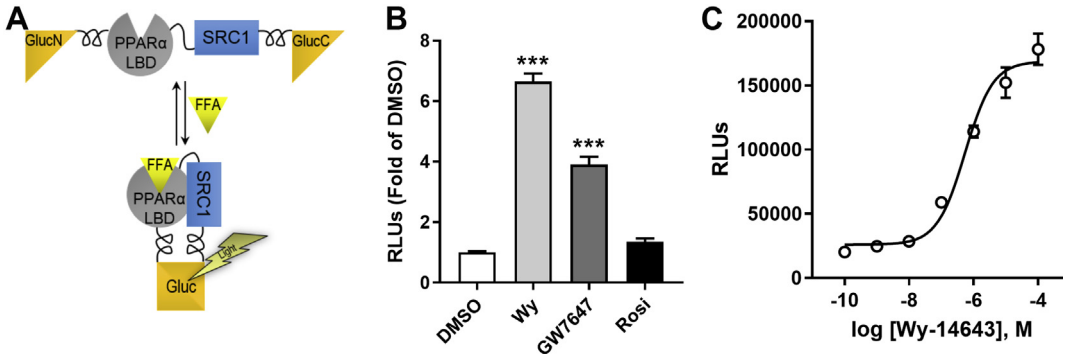

Figure 4: Design of a monomeric luminescent sensor to detect fatty acids. (**A**) Schematic for the design of monomeric luciferase sensor to detect fatty acids. The N-terminal fragment of gaussia luciferase (Gluc) was fused in tandem with the ligand binding domain of PPARα, the LxxLL motif of SRC-1 and the C-terminal domain of Gluc. Fragments were separated by glycine/serine flexible regions. (**B**) Brown pre-adipocytes stably expressing the Gluc fatty acid sensor were treated with the indicated PPAR ligands (Wy 14−643, 100 μM (Wy); GW7647, 1 μM; Rosiglitazone, 1 μM (Rosi)) and the Relative Luminescence Units (RLUs) were determined and expressed as a fold of DMSO. Data are from three independent experiments performed in triplicate. ***$p < 0.001$ indicates a significant effect compared to DMSO as determined by one-way ANOVA. (**C**) Dose response for the PPARα ligand Wy in 293T cells transfected with the Gluc fatty acid sensor. Data are from one experiment performed in quadruplicate and is representative of three independent experiments.

We speculated that the PPARα Gluc sensor would be responsive to exogenous and endogenous FAs, which might provide a useful means of detecting intracellular lipolysis. To test the utility of the sensor we generated a stable BA cell line where the expression of the Gluc FA sensor could be controlled in doxycycline inducible manner. We first examined whether the luciferase sensor could detect exogenous FAs. Addition of oleic acid to cells increased the luciferase signal in a dose-responsive manner (Figure 5A). We next examined whether the

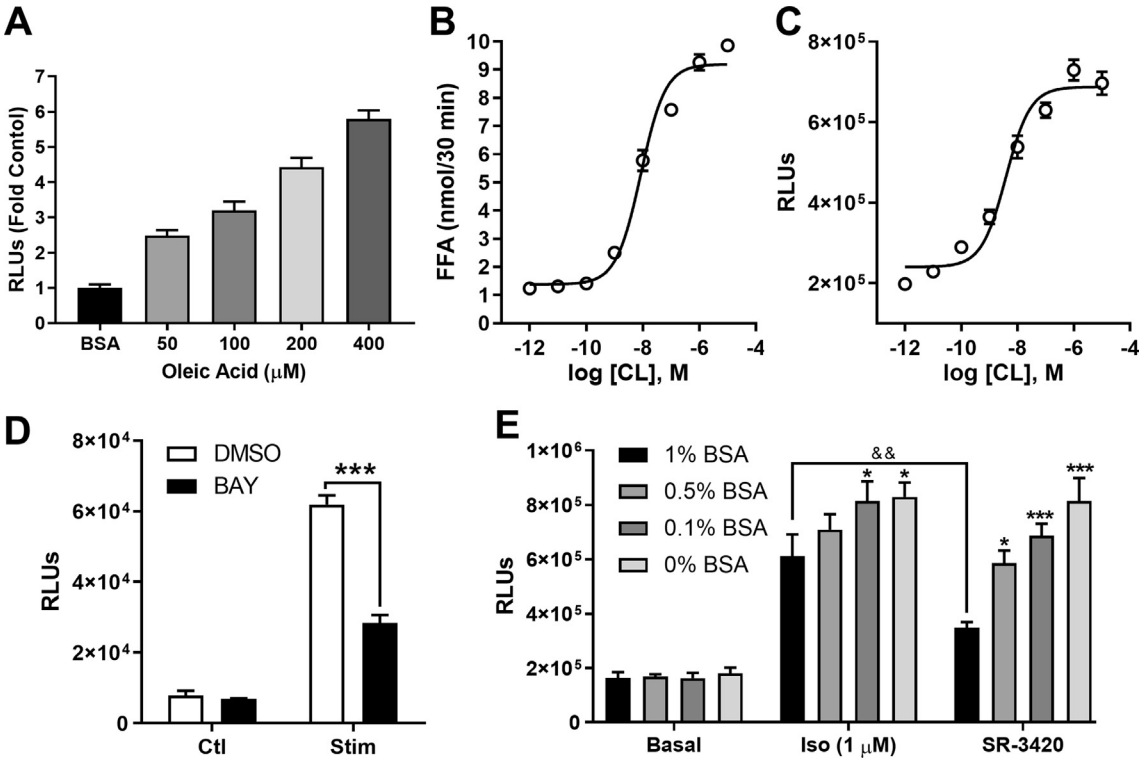

Figure 5: The luminescent fatty acid sensor is sensitive to exogenous and endogenous fatty acids. (**A**) Effect of exogenous fatty acids on the activity of the luminescent fatty acid sensor in undifferentiated pre-brown adipocytes. Cells were treated with different fatty acid concentrations and the Relative Luminescence Units (RLUs) were determined and expressed as a fold of bovine serum albumin (BSA). Dose response for CL-316,243 in differentiated BA as determined by measuring free fatty acids (FFA) in the media (**B**) or RLUs (**C**). (**D**) The Gluc fatty acid sensor is sensitive to inhibition of lipolysis. Differentiated BA were pretreated with the HSL inhibitor (BAY, 5 μM) followed by stimulation with forskolin/IBMX (Stim) and Relative Luminescence Units (RLUs) were determined. ***$p < 0.001$ indicates a significant effect of HSL inhibition as determine by two-way ANOVA with Bonferroni post t-test. (**E**) The Gluc fatty acid sensor detects intracellular fatty acids. Differentiated BA were incubated in the indicated concentrations of bovine serum albumin (BSA) and treated with isoproterenol (Iso, 1 μM) or ABHD5 ligands (SR-3420, 20 μM). *$p < 0.05$, ***$p < 0.001$ indicates a significant effect of BSA concentration compared to 1% BSA within the same treatment group. $^{\&\&}p < 0.01$ indicates a significant difference between Isoproterenol (Iso) and SR-3420 as determined by two-way ANOVA with Bonferroni post t-test. Results are from one experiment performed in sextuplet and is representative of three independent experiments.

 © 2019 The Authors. Published by Elsevier GmbH. This is an open access article under the CC BY-NC-ND license (http://creativecommons.org/licenses/by-nc-nd/4.0/).

luciferase sensor could detect endogenous FAs. BA cells were grown and differentiated, and the expression of the sensor was induced with doxycycline treatment for 24–48 h. Stimulation of lipolysis with the selective β3-adrenoreceptor agonist CL 316,243 (CL) increased lipolysis over a range of doses as determined by the accumulation of extracellular FAs, with a EC_{50} of 8.5 nM (Figure 5B), similar to that previously reported [29]. The luciferase sensor similarly increased reporter activity in a dose responsive manner with a calculated EC_{50} of 3.9 nM, demonstrating the utility of the sensor to detect FAs over a range of lipolysis activation (Figure 5C). We then examined whether the sensor was sensitive to inhibition of lipolysis. Treatment of BA cells with an inhibitor of HSL (BAY), the rate limiting enzyme for the hydrolysis of DAG, resulted in a reduction in luciferase activity when lipolysis was stimulated, but not under basal conditions (Figure 5D). We reasoned that the luminescent sensor was reporting the level of intracellular FAs. To test this, we increased the concentration of intracellular FAs by systematically lowering extracellular bovine serum albumin (BSA), the functional acceptor for FA efflux [30]. As expected, stimulation of the β-adrenergic receptor with Iso increased luminescence in cells incubated with 1% BSA and this effect was increased when the concentration of BSA was lowered to 0.1% and no BSA (0% BSA) (Figure 5E). When lipolysis was directly stimulated with ABHD5 ligand (SR-3420), which by-passes PKA signaling and negative feedback regulation on adenylyl-cyclase [30], the effect was lower compared to Iso in the presence of 1% BSA. However, when the concentration of BSA was lowered to 0.5%, 0.1% and no BSA, SR-3420 had a much greater increase in luciferase activity. Lowering the concentration of BSA in the medium did not affect luciferase activity under basal conditions (Figure 5E). Overall, these data indicate that the luciferase sensor detects production of intracellular FA levels. We also examined whether cells expressing the luciferase reporter were amenable to culture in multi-well format for more high-throughput analysis. Brown pre-adipocyte cells were cultured directly in 96-well clear-bottom white luminescent plates. We first tested the sensitivity of the luciferase sensor to detect FAs of different chain length and saturation. Luminescence increased progressively with greater FA chain length starting with octanoic acid (C8:0), with long chain unsaturated FAs (C18:3, C18:1 and C22:6) demonstrating the greatest increase in luminescence (Figure 6A). Finally, we examined the utility of the FA luminescent sensor to screen for activators and inhibitors of lipolysis in a 96-well plate. The general β-AR agonist isoproterenol and chemical ABHD5 ligands SR-4995, SR-4559, and SR-3420 increased luminescent reporter activity (Figure 6B). The calculated Z' score from this assay was 0.627, indicating that the assay is sufficiently reliable for HTS [31]. The effects of isoproterenol and ABHD5 ligands were partly reduced with HSL inhibition, whereas

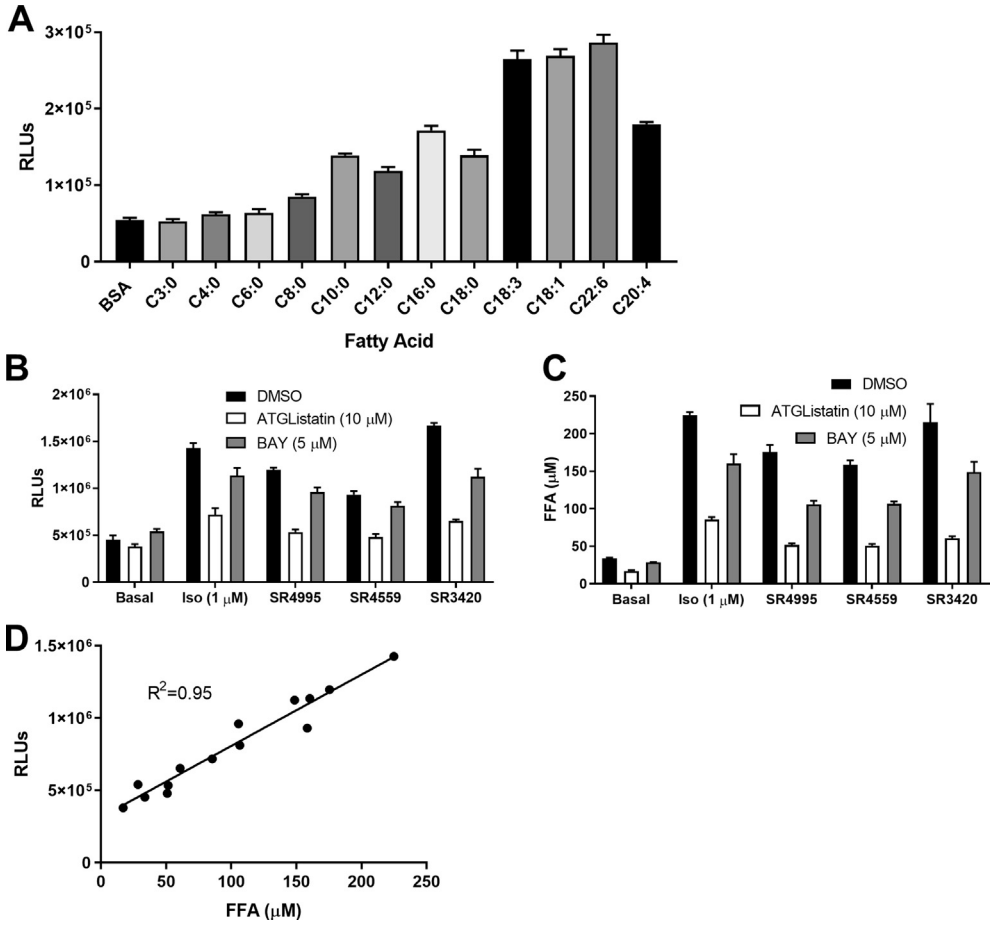

Figure 6: The luminescent fatty acid sensor is amenable to high-throughput analysis. (**A**) Effect of fatty acids of varying chain length and saturation on the luminescent fatty acid sensor in undifferentiated pre-brown adipocytes. Cells grown in 96-well plate were treated with 400 μM of the indicated fatty acids and the Relative Luminescence Units (RLUs) were determined. (**B** and **C**) The luminescent fatty acid sensor is sensitive to various activators and inhibitors of lipolysis. Brown adipocytes were grown and differentiated in white 96-well plates and were then treated with activators (Isoproterenol, 1 μM; SR-4995, SR-4559, SR-3420, 20 μM) and inhibitors of lipolysis for 30 min and the RLUs in cells (**B**) or mobilized free fatty acids (FFA) in media were determined (**C**). (**D**) Correlation between RLUs and FFA from **Figure 6 B** and **D**.

 © 2019 The Authors. Published by Elsevier GmbH. This is an open access article under the CC BY-NC-ND license (http://creativecommons.org/licenses/by-nc-nd/4.0/).

inhibition of ATGL suppressed reporter activity to a greater degree. The efflux of FAs into the extracellular media paralleled the activity of the luciferase reporter (Figure 6C). The relationship between RLUs and FA concentration in this assay showed a linear response with a coefficient of determination of 0.95 (Figure 6D). These data indicate that the luminescent reporter detects lipolysis induced by different modes of chemical activation (receptor or ABHD5) and is amenable to high-throughput analysis.

4. DISCUSSION

Our ability to understand the role of FAs in metabolic homeostasis has been hampered by limitations to image and detect their production in cells. To address this barrier, we have developed genetically-encoded sensors that detect FAs by fluorescent and luminescent means. Using a fluorescent approach, we are able to image the temporal and spatial dynamics of FA trafficking within cells. Furthermore, a luminescent-based monomeric sensor reports intracellular FA levels and is amenable to high-throughput analysis. Using these approaches, we have improved our understanding of how FAs traffic and function within a cell. Our previous work and that of others suggested a role for lipolytic enzymes in providing signaling molecules to regulate gene transcription [10,12,13]; however, the temporal and spatial dynamics for this regulation have not been addressed. Using a fluorescence imaging approach, we took advantage of the ligand-dependent interaction between PPARα and SRC-1 and demonstrate that FAs produced by LDs can traffic to the nucleus within minutes of stimulating lipolysis. The exact mechanism by which FAs traffic from the LDs to the nucleus is currently unknown but might involve lipid binding proteins, such as fatty acid binding protein (FABP) 1 and 4, that traffic the ligands [32,33]. ATGL and HSL are the major lipases in adipocytes; HSL is activated by phosphorylation and translocation to LDs, whereas ATGL is indirectly activated by the release of its co-activator ABHD5 from the scaffold protein PLIN1. Indeed, we found that the kinetics of ATGL and HSL signaling on LDs differed, with HSL activation required for the initial burst of FA release, and ATGL showing a steady increase in FA production on LDs. In contrast, both enzymes had a similar effect on promoting signaling in the nucleus, consistent with both enzyme regulating gene expression [10,12,34]. We also examined the effects of direct ABHD5 activation, independent of PKA stimulation, on lipid signaling. Interestingly, the effect of direct activation of ABHD5 (SR-3420) on FA production on LDs (Figure 2E) was similar to that which was seen when lipolysis was driven only by ATGL (i.e. with HSL inhibition, Figure 2A). However, direct stimulation of ABHD5 resulted in an increase of FAs signaling to the nucleus similar to that of receptor activation (Iso), suggesting that direct stimulation of lipolysis is sufficient to promote signaling to the nucleus. Studies are currently underway to determine the effects of direct stimulation of ABHD5 on gene transcription.

The accumulation of EYFP-SRC1 in the nucleus was somewhat surprising since the exogenous PPARα ligand binding domain was targeted to the LDs, suggesting that SRC-1 was trafficking to the nucleus in a ligand-dependent manner to bind endogenous nuclear receptors. Indeed, the binding of the SRC-1 fragment, lacking an activation domain, suppressed lipolysis-induced transcription of known PPAR target genes. However, pharmacological inhibition of both ATGL and HSL did not completely block the accumulation of EYFP-SRC1 within the nucleus (approximately 80% inhibition), suggesting that PKA-dependent effects on nuclear import or FA trafficking might exist [35,36].

Quantification of FAs typically involves biochemical assays that use colorimetric or fluorescence-based methods to detect extracellular levels. In addition, classical assays for determining PPAR transcriptional activity require transcription/translation events that can take several hours [27]. We reasoned that we could further take advantage of the ligand-dependent interaction between PPARα and SRC-1 to develop a monomeric sensor based on split Gluc. This sensor is able to detect synthetic PPARα ligands and endogenous FAs. Screening of FAs of varying chain length and saturation demonstrates that long-chain unsaturated FAs are potent PPARα ligands [27]. In BAs, the sensor accurately reports known potencies of a β3-AR agonist to stimulate lipolysis and PPARα agonists to induce gene transcription. Culture of BAs stably expressing the sensor in white 96-well format to test activators and inhibitors of lipolysis demonstrates that the sensor is amenable to HTS. Targeting lipolysis is of therapeutic interest, [1,15] and the sensor could be used to screen for novel pharmacological probes that regulate lipolysis and/or PPARα ligands. Finally, expression of the luciferase sensor in transgenic animals could be used as an in vivo probe to monitor dynamics of FA production, uptake, and clearance, thereby improving our understanding of FA metabolism and their potential lipotoxic effects.

5. CONCLUSIONS

In summary, we have developed genetically-encoded sensors to determine the temporal and spatial dynamics of FA production, that typically would not be possible using more conventional approaches. Given the increased interest in studying FA metabolism and ever-expanding obesity epidemic confronting our society, the use of these sensors will further improve our understanding of FA trafficking and metabolism.

AUTHOR CONTRIBUTIONS

E.P.M. and J.G.G. conceived the experiments. E.P.M. and J.G.G. designed the experiments. E.P.M, H.Z., A.Y., and L.Z conducted the experiments. E.P.M. and J.G.G. analyzed the data and E.P.M. and J.G.G. wrote and edited the manuscript. All authors read the manuscript and approved the final version.

ACKNOWLEDGEMENTS

This work was supported by NIH grants K99-DK114471 to E.P.M, and DK76629, DK105963, and R21DK091741 to J.G.G. The funding agencies were not involved in the study design, collection analysis and interpretation of data; in the writing of the report; and in the decision to submit the article for publication.

CONFLICT OF INTEREST

The authors declare no competing interests. The authors (Emilio Mottillo, Huamei Zhang, Alexander Yang, Li Zhou, James Granneman) wish to confirm that there are no known conflicts of interest associated with the manuscript entitled "Genetically-encoded sensors to detect fatty acid production and trafficking" and there has been no significant financial support for this work that could have influenced its outcome.

APPENDIX A. SUPPLEMENTARY DATA

Supplementary data to this article can be found online at https://doi.org/10.1016/j.molmet.2019.08.012.

REFERENCES

[1] Zechner, R., Zimmermann, R., Eichmann, T.O., Kohlwein, S.D., Haemmerle, G., Lass, A., et al., 2012. FAT SIGNALS — lipases and lipolysis in lipid metabolism

 © 2019 The Authors. Published by Elsevier GmbH. This is an open access article under the CC BY-NC-ND license (http://creativecommons.org/licenses/by-nc-nd/4.0/).

and signaling. Cell Metabolism 15(3):279–291. https://doi.org/10.1016/j.cmet.2011.12.018.

[2] Unger, R.H., Scherer, P.E., 2010. Gluttony, sloth and the metabolic syndrome: a roadmap to lipotoxicity. Trends in Endocrinology and Metabolism 21(6):345–352. https://doi.org/10.1016/j.tem.2010.01.009.

[3] Unger, R.H., 2002. Lipotoxic diseases. Annual Review of Medicine 53(1):319–336.

[4] Schulze, P.C., Drosatos, K., Goldberg, I.J., 2016. Lipid use and misuse by the heart. Circulation Research 118(11):1736–1751. https://doi.org/10.1161/CIRCRESAHA.116.306842.

[5] Walther, T.C., Chung, J., Jr, R.V.F., 2017. Lipid droplet biogenesis. Annual Review of Cell and Developmental Biology 33(1). https://doi.org/10.1146/annurev-cellbio-100616-060608 null.

[6] Granneman, J.G., Moore, H.-P.H., 2008. Location, location: protein trafficking and lipolysis in adipocytes. Trends in Endocrinology and Metabolism 19(1):3–9. https://doi.org/10.1016/j.tem.2007.10.006.

[7] Shabalina, I.G., Jacobsson, A., Cannon, B., Nedergaard, J., 2004. Native UCP1 displays simple competitive kinetics between the regulators purine nucleotides and fatty acids. Journal of Biological Chemistry 279(37):38236–38248. https://doi.org/10.1074/jbc.M402375200.

[8] Nicholls, D.G., Locke, R.M., 1984. Thermogenic mechanisms in brown fat. Physiological Reviews 64(1):1–64.

[9] Fedorenko, A., Lishko, P.V., Kirichok, Y., 2012. Mechanism of fatty-acid-dependent UCP1 uncoupling in brown fat mitochondria. Cell 151(2):400–413. https://doi.org/10.1016/j.cell.2012.09.010.

[10] Mottillo, E.P., Bloch, A.E., Leff, T., Granneman, J.G., 2012. Lipolytic products activate peroxisome proliferator-activated receptor (PPAR) and in brown adipocytes to match fatty acid oxidation with supply. Journal of Biological Chemistry 287(30):25038–25048. https://doi.org/10.1074/jbc.M112.374041.

[11] Ahmadian, M., Abbott, M.J., Tang, T., Hudak, C.S.S., Kim, Y., Bruss, M., et al., 2011. Desnutrin/ATGL is regulated by AMPK and is required for a Brown adipose phenotype. Cell Metabolism 13(6):739–748. https://doi.org/10.1016/j.cmet.2011.05.002.

[12] Haemmerle, G., Moustafa, T., Woelkart, G., Büttner, S., Schmidt, A., van de Weijer, T., et al., 2011. ATGL-mediated fat catabolism regulates cardiac mitochondrial function via PPAR-α and PGC-1. Nature Medicine 17(9):1076–1085. https://doi.org/10.1038/nm.2439.

[13] Ong, K.T., Mashek, M.T., Bu, S.Y., Greenberg, A.S., Mashek, D.G., 2011. Adipose triglyceride lipase is a major hepatic lipase that regulates triacylglycerol turnover and fatty acid signaling and partitioning. Hepatology 53(1):116–126. https://doi.org/10.1002/hep.24006.

[14] Kim, S.B., Sato, M., Tao, H., 2009. Split Gaussia luciferase-based bioluminescence template for tracing protein dynamics in living cells. Analytical Chemistry 81(1):67–74. https://doi.org/10.1021/ac801658y.

[15] Sanders, M.A., Madoux, F., Mladenovic, L., Zhang, H., Ye, X., Angrish, M., et al., 2015. Endogenous and synthetic ABHD5 ligands regulate ABHD5-perilipin interactions and lipolysis in fat and muscle. Cell Metabolism 22(5):851–860. https://doi.org/10.1016/j.cmet.2015.08.023.

[16] Yang, A., Mottillo, E.P., Mladenovic-Lucas, L., Zhou, L., Granneman, J.G., 2019. Dynamic interactions of ABHD5 with PNPLA3 regulate triacylglycerol metabolism in brown adipocytes. Nature Metabolism, 1. https://doi.org/10.1038/s42255-019-0066-3.

[17] Livak, K.J., Schmittgen, T.D., 2001. Analysis of relative gene expression data using real-time quantitative PCR and the 2(-Delta Delta C(T)) Method. Methods (San Diego, Calif.) 25(4):402–408. https://doi.org/10.1006/meth.2001.1262.

[18] Maguire, C.A., Deliolanis, N.C., Pike, L., Niers, J.M., Tjon-Kon-Fat, L.-A., Sena-Esteves, M., et al., 2009. Gaussia luciferase variant for high-throughput functional screening applications. Analytical Chemistry 81(16):7102–7106. https://doi.org/10.1021/ac901234r.

[19] Lass, A., Zimmermann, R., Haemmerle, G., Riederer, M., Schoiswohl, G., Schweiger, M., et al., 2006. Adipose triglyceride lipase-mediated lipolysis of cellular fat stores is activated by CGI-58 and defective in Chanarin-Dorfman syndrome. Cell Metabolism 3(5):309–319. https://doi.org/10.1016/j.cmet.2006.03.005.

[20] Yamaguchi, T., Omatsu, N., Matsushita, S., Osumi, T., 2004. CGI-58 interacts with perilipin and is localized to lipid droplets: possible involvement of CGI-58 mislocalization in Chanarin-Dorfman syndrome. Journal of Biological Chemistry 279(29):30490–30497. https://doi.org/10.1074/jbc.M403920200.

[21] Moore, H.-P.H., Silver, R.B., Mottillo, E.P., Bernlohr, D.A., Granneman, J.G., 2005. Perilipin targets a novel pool of lipid droplets for lipolytic attack by hormone-sensitive lipase. Journal of Biological Chemistry 280(52):43109–43120. https://doi.org/10.1074/jbc.M506336200.

[22] Su, C.-L., Sztalryd, C., Contreras, J.A., Holm, C., Kimmel, A.R., Londos, C., 2003. Mutational analysis of the hormone-sensitive lipase translocation reaction in adipocytes. Journal of Biological Chemistry 278(44):43615–43619. https://doi.org/10.1074/jbc.M301809200.

[23] Claus, T.H., Lowe, D.B., Liang, Y., Salhanick, A.I., Lubeski, C.K., Yang, L., et al., 2005. Specific inhibition of hormone-sensitive lipase improves lipid profile while reducing plasma glucose. Journal of Pharmacology and Experimental Therapeutics 315(3):1396–1402. https://doi.org/10.1124/jpet.105.086926.

[24] Mayer, N., Schweiger, M., Romauch, M., Grabner, G.F., Eichmann, T.O., Fuchs, E., et al., 2013. Development of small molecule inhibitors targeting adipose triglyceride lipase. Nature Chemical Biology 9(12). https://doi.org/10.1038/nchembio.1359.

[25] Rondini, E.A., Mladenovic-Lucas, L., Roush, W.R., Halvorsen, G.T., Green, A.E., Granneman, J.G., 2017. Novel pharmacological probes reveal ABHD5 as a locus of lipolysis control in white and brown adipocytes. Journal of Pharmacology and Experimental Therapeutics 363(3):367–376. https://doi.org/10.1124/jpet.117.243253.

[26] Kim, S.B., Sato, M., Tao, H., 2009. Genetically encoded bioluminescent indicators for stress hormones. Analytical Chemistry 81(10):3760–3768. https://doi.org/10.1021/ac802674w.

[27] Forman, B.M., Chen, J., Evans, R.M., 1997. Hypolipidemic drugs, polyunsaturated fatty acids, and eicosanoids are ligands for peroxisome proliferator-activated receptors α and δ. Proceedings of the National Academy of Sciences 94(9):4312–4317.

[28] Hsu, M.H., Palmer, C.N., Griffin, K.J., Johnson, E.F., 1995. A single amino acid change in the mouse peroxisome proliferator-activated receptor alpha alters transcriptional responses to peroxisome proliferators. Molecular Pharmacology 48(3):559–567.

[29] Atgié, C., D'Allaire, F., Bukowiecki, L.J., 1997. Role of β1-and β3-adrenoceptors in the regulation of lipolysis and thermogenesis in rat brown adipocytes. American Journal of Physiology-Cell Physiology 273(4):C1136–C1142.

[30] Mottillo, E.P., Granneman, J.G., 2011. Intracellular fatty acids suppress beta-adrenergic induction of PKA-targeted gene expression in white adipocytes. American Journal of Physiology. Endocrinology and Metabolism 301(1):E122–E131. https://doi.org/10.1152/ajpendo.00039.2011.

[31] Zhang, Chung, Oldenburg, 1999. A simple statistical parameter for use in evaluation and validation of high throughput screening assays. Journal of Biomolecular Screening 4(2):67–73. https://doi.org/10.1177/108705719900400206.

[32] Hofer, P., Boeszoermenyi, A., Jaeger, D., Feiler, U., Arthanari, H., Mayer, N., et al., 2015. Fatty acid-binding proteins interact with comparative gene identification-58 linking lipolysis with lipid ligand shuttling. Journal of Biological Chemistry 290(30):18438–18453. https://doi.org/10.1074/jbc.M114.628958.

[33] Hostetler, H.A., McIntosh, A.L., Atshaves, B.P., Storey, S.M., Payne, H.R., Kier, A.B., et al., 2009. L-FABP directly interacts with PPARalpha in cultured primary hepatocytes. Journal of Lipid Research 50(8):1663–1675. https://doi.org/10.1194/jlr.M900058-JLR200.

 © 2019 The Authors. Published by Elsevier GmbH. This is an open access article under the CC BY-NC-ND license (http://creativecommons.org/licenses/by-nc-nd/4.0/).

[34] Shen, W.-J., Yu, Z., Patel, S., Jue, D., Liu, L.-F., Kraemer, F.B., 2011. Hormone-sensitive lipase modulates adipose metabolism through PPARgamma. Biochimica et Biophysica Acta 1811(1):9–16. https://doi.org/10.1016/j.bbalip.2010.10.001.

[35] Chang, C.-W.J., Lee, L., Yu, D., Dao, K., Bossuyt, J., Bers, D.M., 2013. Acute beta-adrenergic activation triggers nuclear import of histone deacetylase 5 and delays G(q)-induced transcriptional activation. The Journal of Biological Chemistry 288(1):192–204. https://doi.org/10.1074/jbc.M112.382358.

[36] Liu, X., Lin, W., Shi, X., Davies, R.G., Wagstaff, K.M., Tao, T., et al., 2018. PKA-site phosphorylation of importin13 regulates its subcellular localization and nuclear transport function. The Biochemical Journal 475(16):2699–2712. https://doi.org/10.1042/BCJ20180082.

 © 2019 The Authors. Published by Elsevier GmbH. This is an open access article under the CC BY-NC-ND license (http://creativecommons.org/licenses/by-nc-nd/4.0/).